

## Vibrational Spectroscopic Studies of Trivalent Hexa-aqua-cations: Single-crystal Raman Spectra between 275 and 1 200 $\text{cm}^{-1}$ of the Caesium Alums of Titanium, Vanadium, Chromium, Iron, Gallium, and Indium †

Stephen P. Best,\* James K. Beattie, and Robert S. Armstrong  
School of Chemistry, University of Sydney, Sydney, New South Wales, 2006, Australia

Oriented single-crystal Raman spectra have been recorded at 80 or 90 K for  $\text{CsM}(\text{SO}_4)_2 \cdot 12\text{H}_2\text{O}$  ( $M = \text{Ti, V, Cr, Fe, Ga, or In}$ ),  $\text{CsM}(\text{SeO}_4)_2 \cdot 12\text{H}_2\text{O}$  ( $M = \text{Cr or Fe}$ ), and  $\text{CsFe}(\text{SO}_4)_2 \cdot 12\text{D}_2\text{O}$ . A complete assignment of the spectra between 275 and 1 200  $\text{cm}^{-1}$  has been made. The total symmetric metal–water stretching modes of the trivalent hexa-aqua-cations occur at 517 (Ti), 525 (V), 540 (Cr), 523 (Fe), 537 (Ga), and 505  $\text{cm}^{-1}$  (In), significantly higher than values previously reported. The wavenumbers of these modes vary with the reciprocal of the metal(III)–water bond lengths.

Despite the importance of the trivalent hexa-aqua-cation in aqueous chemistry the vibrational spectroscopy of this species remains poorly defined. The wavenumbers of the totally symmetric stretching mode for all but the  $[\text{Al}(\text{OH}_2)_6]^{3+}$  cation remain uncertain.

A comparative study of trivalent hexa-aqua-cations in well defined and similar sites enables an unambiguous determination and assignment of their vibrational frequencies. The caesium alums provide a lattice wherein a wide range of trivalent hexa-aqua-cations can be isomorphously replaced with little change to the lattice.<sup>1</sup> A recent single-crystal Raman study on a series of caesium aluminium alums<sup>2</sup> has demonstrated that despite the size of the unit cell (192 atoms) the problem is vibrationally tractable. In this paper we present the first comparative study of the Raman-active modes of a wide range of trivalent hexa-aqua-cations.

Infrared spectroscopy has been used to study various alums.<sup>3–6</sup> The information obtained is complementary to the Raman data and provides identification of the Raman-inactive  $\nu_3$  and  $\nu_4$  modes of the trivalent hexa-aqua-cation. These studies have been mostly carried out at room temperature on Nujol mulls; consequently the assignments lack the rigour of an oriented single-crystal Raman study.

Raman solution studies of the trivalent metal cations have been reported for Al,<sup>7,8</sup> Ga,<sup>9</sup> In,<sup>9</sup> Cr,<sup>10</sup> and Fe.<sup>11</sup> Polarised bands are found between 400 and 530  $\text{cm}^{-1}$ . Although the assignment of these bands to vibrations of aquated metal cations is likely, the presence of the hexa-aqua-cation can only be certain for aluminium where reliable assignments of the vibrational modes of the aluminium hexa-aqua-cation are available.<sup>2,12,13</sup> It is probable that in many of these studies inner-sphere co-ordination of anions or the presence of hydroxo-species complicates the spectrum.

We have chosen the series  $\text{CsFe}(\text{SO}_4)_2 \cdot 12\text{H}_2\text{O}$ ,  $\text{CsFe}(\text{SeO}_4)_2 \cdot 12\text{H}_2\text{O}$ , and  $\text{CsFe}(\text{SO}_4)_2 \cdot 12\text{D}_2\text{O}$  to make our assignments of the  $[\text{Fe}(\text{OH}_2)_6]^{3+}$  species and to confirm that the analysis of these spectra is consistent with that of the aluminium alums.<sup>2</sup> The Raman spectra of  $\text{CsM}(\text{SO}_4)_2 \cdot 12\text{H}_2\text{O}$  ( $M = \text{Cr, Ga, In, V, or Ti}$ ) and  $\text{CsCr}(\text{SeO}_4)_2 \cdot 12\text{H}_2\text{O}$  are assigned with the aid of the analysis of the aluminium and iron alums.

### Experimental

The caesium sulphate hydrate alums were prepared by using the methods described in the literature (Ga,<sup>1</sup> In,<sup>1</sup> Ti,<sup>3</sup> V,<sup>14</sup> Cr,<sup>14</sup> and Fe<sup>14</sup>). Large single crystals were prepared from solutions of sulphuric acid (1 mol  $\text{dm}^{-3}$ ) by the controlled deposition of the growth material onto a suspended seed crystal. The mass transport was accomplished by maintaining a thermal gradient over the apparatus.

The alum  $\text{CsCr}(\text{SeO}_4)_2 \cdot 12\text{H}_2\text{O}$  was prepared by the dissolution of stoichiometric quantities of chromium(VI) oxide and caesium carbonate in selenic acid (1 mol  $\text{dm}^{-3}$ ) followed by the addition of an excess of hydrogen peroxide (30% w/v) with heating. The excess of peroxide was decomposed by heating and the solution was allowed to cool, allowing crystallisation of the alum. Following recrystallisation from selenic acid (1 mol  $\text{dm}^{-3}$ ) large single crystals were grown from the same solvent using the technique outlined above.

The alum  $\text{CsFe}(\text{SeO}_4)_2 \cdot 12\text{H}_2\text{O}$  was prepared by the dissolution of freshly prepared iron(III) hydroxide in selenic acid (1 mol  $\text{dm}^{-3}$ ) followed by the addition of a stoichiometric quantity of caesium carbonate. The resulting solid was recrystallised from selenic acid (1 mol  $\text{dm}^{-3}$ ) and large single crystals were grown from the same solvent using the technique outlined above.

The alum  $\text{CsFe}(\text{SO}_4)_2 \cdot 12\text{D}_2\text{O}$  was prepared and handled under a dry atmosphere of either argon or nitrogen. Stoichiometric quantities of anhydrous iron(III) chloride and caesium sulphate were dissolved in  $[\text{D}_2\text{H}_2]$  sulphuric acid (1 mol  $\text{dm}^{-3}$ ). An equimolar quantity, based on chloride, of freshly prepared silver carbonate was added and the solution maintained close to 350 K for 1 h. The slurry was filtered warm before any crystallisation of the alum was evident. The solid was recrystallised from  $[\text{D}_2\text{H}_2]$  sulphuric acid and large single crystals were grown from the same solvent using the technique outlined above.

For each alum the crystallographic axes could be deduced from the crystal morphology which was predominantly octahedral with varying degrees of edge and corner truncation. For crystals with extensive truncation of the octahedral faces it was necessary to measure the interfacial angles, using an optical goniometer, in order to establish unambiguously the orientation of the crystallographic axes.

Experiments of the type  $X'(\alpha\beta)Z$ ,  $Z(\alpha\beta)X'$ , or  $X'(\alpha\beta)Y'$ , where  $X'$ ,  $Y'$  are related to  $X$ ,  $Y$  by a rotation about  $Z$  of  $\frac{\pi}{2}$  radians, were chosen since a complete data set could be obtained in this way without reorientation of the crystal. The choice of the excitation and collection directions was made by

\* Present address: Chemistry Department, University College London, 20 Gordon Street, London WC1H 0AJ.

† Supplementary data available (No. SUP 56047, 8 pp.): single-crystal Raman spectra. See Instructions for Authors, *J. Chem. Soc., Dalton Trans.*, 1984, Issue 1, pp. xvii–xix.

**Table 1.** Raman activities for the different scattering experiments

Tensor Component	Activity
$(X'X'), (Y'Y')$	$A_g + F_g + E_g/4$
$(ZZ)$	$A_g + E_g$
$(X'Y')$	$E_g$
$(X'Z), (Y'Z)$	$F_g$

$X', Y'$  are related to  $X, Y$  by a rotation of  $\frac{\pi}{4}$  radians about  $Z$ . The scattering tensor is symmetric.

considering the shape of the crystal and by making use of an area which was optically clear and free of crystal defects. The activities of the Raman bands for each of the scattering experiments are given in Table 1.

The crystals were excited using Spectra Physics model 164 Ar<sup>+</sup> and Kr<sup>+</sup> lasers. The choice of the appropriate laser line was dependent on the absorption spectrum of the crystal. The details of the spectrometer were given previously.<sup>2</sup> A Commodore CBM model 4032 minicomputer was used to control the monochromator and to initiate readings and collect data from the photon counter. Calibration and temperature measurement for all spectra were accomplished using Stokes and anti-Stokes peaks. The linearity of the wavenumber scale was checked using plasma emissions of the Ar<sup>+</sup> and Kr<sup>+</sup> lasers.

## Results

The caesium alums are an isomorphous series of cubic double salts conforming to the space group  $Pa\bar{3}$ . The molecular groupings within the unit cell have been satisfactorily identified<sup>2</sup> and are: (i) the trivalent hexa-aqua-cation, found on a site of  $S_6$  symmetry; (ii) the sulphate or selenate anions, found on sites of  $C_3$  symmetry; and (iii) the monovalent cation with its more loosely bound co-ordination sphere of six water molecules, found on a site of  $S_6$  symmetry. The factor-group analysis (f.g.a.) is identical for all the alums and is given in Table 1 of ref. 2.

From the spectra published on the analogous series of aluminium alums,<sup>2</sup> the region 275–1 200 cm<sup>-1</sup> is expected to contain vibrations of the four internal sulphate modes, the three Raman-active internal modes of the trivalent hexa-aqua-cation, and six external modes of co-ordinated water. Schematic representations of the internal modes of the octahedral MX<sub>6</sub> and tetrahedral AB<sub>4</sub> species may be found in many vibrational texts; for example, see ref. 15. Representations of the external modes may also be found in the literature.<sup>16</sup>

For each of the alums studied, spectra were recorded over the region 10–1 200 cm<sup>-1</sup>. In the region between 10 and 275 cm<sup>-1</sup>, f.g.a. predicts 6  $A_g$  + 6  $E_g$  + 18  $F_g$  bands. In each case six bands of  $E_g$  symmetry can be identified, although often only five  $A_g$  components and fewer than the number of  $F_g$  components expected are found. The same adherence to the f.g.a. is found for the caesium aluminium alums<sup>2</sup> and supports our interpretation of the spectrum. The spectra recorded between 10 and 275 cm<sup>-1</sup> will be published subsequently.

Spectra were recorded at close to liquid-nitrogen temperature because many of the crystals are highly coloured and thermal decomposition occurred on excitation at room temperature. The narrower full-widths at half-height (f.w.h.h.) of bands found at this low temperature also allow a more precise determination of the vibrational frequencies, particularly with the external modes which are weak and broad at room temperature. For CsTi(SO<sub>4</sub>)<sub>2</sub>·12H<sub>2</sub>O a strong band of  $E_g$

symmetry is found at 38 cm<sup>-1</sup> with a f.w.h.h. of 12 cm<sup>-1</sup>. This band is much broader than the corresponding bands found for the other alums (ca. 4 cm<sup>-1</sup>). At room temperature the corresponding band is found at 39 cm<sup>-1</sup> but with a f.w.h.h. of 8 cm<sup>-1</sup>. The anomalous increase in the f.w.h.h. with decreasing temperature is consistent with the behaviour of a soft mode, which indicates the onset of a phase transition below 80 K. The remaining bands in the spectrum are found with larger f.w.h.h. than the corresponding bands in the other spectra. However, the number of bands found for each symmetry species is in agreement with that expected, thus allowing reliable assignments of the spectra. For all the other alums studied no bands are found which are indicative of a phase transition.

Spectra of CsFe(SO<sub>4</sub>)<sub>2</sub>·12H<sub>2</sub>O and CsFe(SO<sub>4</sub>)<sub>2</sub>·12D<sub>2</sub>O were also recorded in the region 1 200–4 000 cm<sup>-1</sup>. An estimate of the isotopic purity of the latter of at least 98% can be made by comparison between the intensities of the OH and OD stretches. Because of the high level of isotopic purity achieved the occurrence of bands of CsFe(SO<sub>4</sub>)<sub>2</sub>·12D<sub>2</sub>O in the region 275–1 200 cm<sup>-1</sup> due to isotopic impurity can be neglected.

The identification of weak bands of  $A_g$  symmetry in the mixed-component spectra or of weak  $E_g$  or  $F_g$  bands close to the leakage of strong bands of different symmetry in the single-component spectra has been aided by the following techniques: (i) scaling the appropriate spectra and subtracting such that any obvious leakage is eliminated and no negative peaks occur and (ii) fitting the strong bands of different symmetry to Lorentzian-Gaussian bandshapes and subtracting the appropriately scaled bandshape.<sup>17</sup> The latter technique is useful where there is leakage of more than one band and the weak component to be identified is close to only one of the offending bands. The unaltered band then provides an internal reference against which significant deviations can be measured.

(A) *Assignment of the Spectra of CsFe(SO<sub>4</sub>)<sub>2</sub>·12H<sub>2</sub>O, CsFe(SeO<sub>4</sub>)<sub>2</sub>·12H<sub>2</sub>O, and CsFe(SO<sub>4</sub>)<sub>2</sub>·12D<sub>2</sub>O over the Region 275–1 200 cm<sup>-1</sup>.*—In this region of the spectrum 11  $A_g$  + 11  $E_g$  + 33  $F_g$  bands should be found. For CsFe(SO<sub>4</sub>)<sub>2</sub>·12H<sub>2</sub>O, 6  $A_g$  + 11  $E_g$  + 19  $F_g$  bands are observed, for CsFe(SeO<sub>4</sub>)<sub>2</sub>·12H<sub>2</sub>O 9  $A_g$  + 11  $E_g$  + 21  $F_g$ , and for CsFe(SO<sub>4</sub>)<sub>2</sub>·12D<sub>2</sub>O 6  $A_g$  + 11  $E_g$  + 17  $F_g$  bands. This is similar to the results for the aluminium alums<sup>2</sup> where all 11  $E_g$  bands derived from the expected modes but fewer than the expected numbers of  $A_g$  and  $F_g$  bands were found.

(i) *Internal modes of [Fe(OH<sub>2</sub>)<sub>6</sub>]<sup>3+</sup> and [Fe(OD<sub>2</sub>)<sub>6</sub>]<sup>3+</sup>.*  $\nu_1(\text{FeO}_6)$ . The f.g.a. indicates that one band of  $A_g$  symmetry and one of  $F_g$  symmetry should result from this mode. The most pronounced difference between the spectrum of CsFe(SO<sub>4</sub>)<sub>2</sub>·12H<sub>2</sub>O and CsAl(SO<sub>4</sub>)<sub>2</sub>·12H<sub>2</sub>O is the occurrence of a strong band of  $A_g$  symmetry at 523 cm<sup>-1</sup>. In the spectrum of CsFe(SeO<sub>4</sub>)<sub>2</sub>·12H<sub>2</sub>O a band of  $A_g$  symmetry is found with comparable intensity at 523 cm<sup>-1</sup>. This band shifts to 500 cm<sup>-1</sup> on deuteration, the band being easily identified from its high intensity (Figures 1 and 3). The ratio  $\nu_D/\nu_H$  is 0.95, consistent with the calculated value of 0.949 for the  $\nu_1(\text{FeO}_6)$  mode.

The  $F_g$  component of the  $\nu_1(\text{FeO}_6)$  mode should be found close to the  $A_g$  component. For CsFe(SO<sub>4</sub>)<sub>2</sub>·12H<sub>2</sub>O a band of  $F_g$  symmetry is found at 540 cm<sup>-1</sup>. The assignment of this band to the  $\nu_1(\text{FeO}_6)$  mode is excluded for two reasons: (i) there is a band of  $E_g$  symmetry with a similar bandshape close by at 542 cm<sup>-1</sup>, and both this and the  $F_g$  bands shift on deuteration with the ratio  $\nu_D/\nu_H$  of 0.725 ± 0.01 in excellent agreement with the ratio expected for an external mode (0.723), and (ii) there is no equivalent band of  $F_g$  symmetry in the spectrum of the deuterate. Thus although the  $A_g$  component of the  $\nu_1(\text{FeO}_6)$  mode is very strong, the  $F_g$  component is very weak

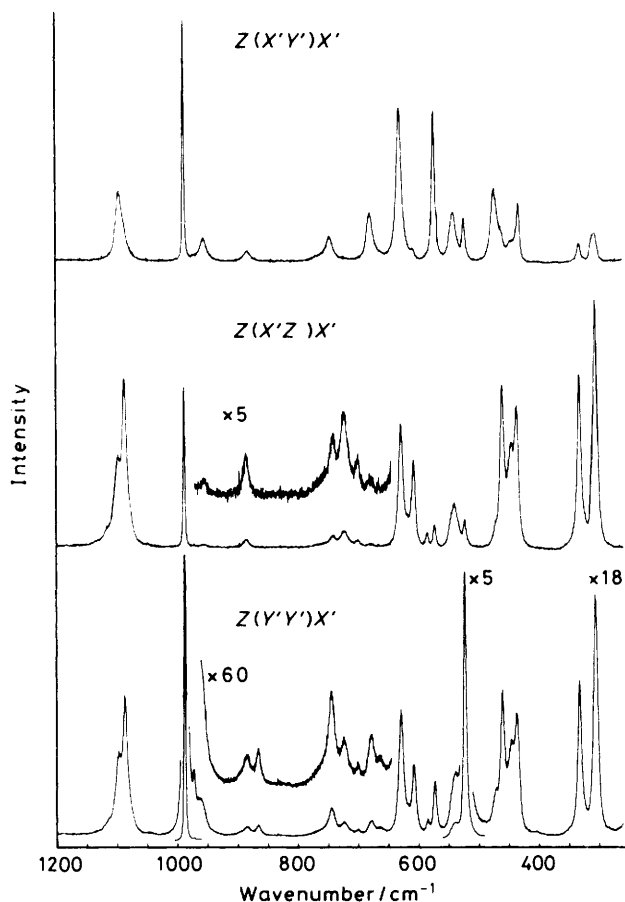


Figure 1. Single-crystal Raman spectra of  $\text{CsFe}(\text{SO}_4)_2 \cdot 12\text{H}_2\text{O}$  at 80 K. Spectral bandwidth  $2.6 \text{ cm}^{-1}$  at  $600 \text{ cm}^{-1}$ ; step size  $0.4 \text{ cm}^{-1}$ ; 35-mW, 487.98-nm radiation at sample. Sensitivities:  $Z(Y'Y')X'$ , 75 000;  $Z(X'Z)X'$ , 2 627; and  $Z(X'Y')X'$ , 2 990 counts  $\text{s}^{-1}$

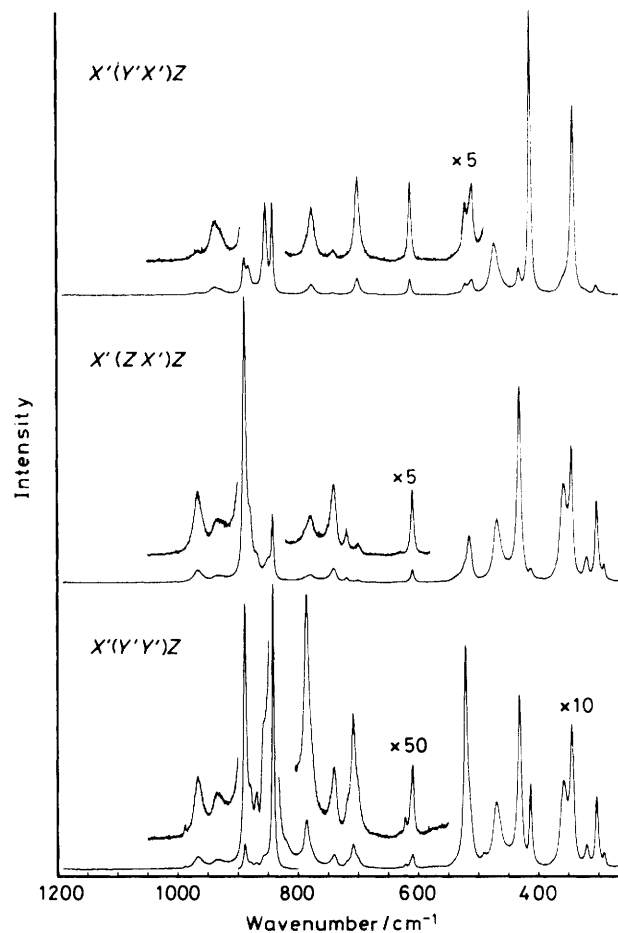


Figure 2. Single-crystal Raman spectra of  $\text{CsFe}(\text{SeO}_4)_2 \cdot 12\text{H}_2\text{O}$  at 80 K. Spectral bandwidth  $1.9 \text{ cm}^{-1}$  at  $600 \text{ cm}^{-1}$ ; step size  $0.4 \text{ cm}^{-1}$ ; 50-mW, 487.98-nm radiation at sample. Sensitivities:  $X'(Y'Y')Z$ , 94 500;  $X'(ZX')Z$ , 7 650;  $X'(Y'X')Z$ , 6 480 counts  $\text{s}^{-1}$

in all the caesium iron(III) alums studied. This behaviour is similar to that of the totally symmetric stretches of sulphate and selenate where the intensity is found to be concentrated in the  $A_g$  component (see Figures 1–3).

The assignment of the  $A_g$  band at  $523 \text{ cm}^{-1}$  for  $\text{CsFe}(\text{SO}_4)_2 \cdot 12\text{H}_2\text{O}$  to  $\nu_1(\text{FeO}_6)$  is unambiguous and follows from the shift found on deuteration and the constancy of the band upon substitution of sulphate for selenate. In the aluminium alums the  $\nu_1(\text{AlO}_6)$  mode is found at  $542 \text{ cm}^{-1}$ . This energy difference reflects the bond-strength difference indicated by the bond length of  $1.877 \text{ \AA}$  for  $\text{Al}-\text{OH}_2$ ,  $0.078 \text{ \AA}$  shorter than  $\text{Fe}-\text{OH}_2$ .<sup>1</sup> The intensities of the respective bands are markedly different with the  $\nu_1(\text{FeO}_6)$  mode being very strong and the  $\nu_1(\text{AlO}_6)$  mode weak. Since the  $A_g$  component of the  $\nu_1(\text{FeO}_6)$  mode is so strong it is possible to examine the extent of coupling of this mode to other modes of similar energy. The occurrence of coupling would result in both energy shifts and intensity borrowing; therefore any significant coupling requires the observation of modes of  $A_g$  symmetry of unusually large intensity compared to those bands found in  $\text{CsAl}(\text{SO}_4)_2 \cdot 12\text{H}_2\text{O}$  where the  $A_g$  component is weak. There are no bands of  $A_g$  symmetry having intensities very different from those found for  $\text{CsAl}(\text{SO}_4)_2 \cdot 12\text{H}_2\text{O}$  in the region near the  $\nu_1(\text{MO}_6)$  modes. Hence we can exclude the presence of strong coupling between the  $\nu_1(\text{FeO}_6)$  mode and the other modes nearby.

$\nu_2(\text{FeO}_6)$ . The upper energy limit for the  $\nu_2(\text{FeO}_6)$  mode

follows from the order of the skeletal modes of a regular octahedral species which is determined by the dynamic equations. These require that this mode lies to lower energy than the  $\nu_1(\text{FeO}_6)$  mode<sup>12</sup> found at  $523 \text{ cm}^{-1}$ . A lower limit of  $400 \text{ cm}^{-1}$  is obtained by comparison with the spectra of the caesium aluminium alums where the uncoupled  $\nu_2(\text{AlO}_6)$  mode is found at  $473 \text{ cm}^{-1}$ ,<sup>2</sup> and by consideration of the relative strengths of the  $\text{Al}-\text{OH}_2$  and the  $\text{Fe}-\text{OH}_2$  bonds. Spectra of aluminium sulphate alums<sup>2,13</sup> and of alkaline-earth-metal sulphates<sup>18,19</sup> indicate that the  $\nu_2(\text{SO}_4)$  mode will also be found in this region of the spectrum. For  $\text{CsFe}(\text{SO}_4)_2 \cdot 12\text{H}_2\text{O}$  bands are found at  $432$  and  $473$  ( $E_g$ ) and  $436$ ,  $445$ , and  $460 \text{ cm}^{-1}$  ( $F_g$ ).

Since all the modes of  $E_g$  symmetry have been found and only two occur between  $523$  and  $400 \text{ cm}^{-1}$  these must be the  $\nu_2(\text{FeO}_6)$  and the  $\nu_2(\text{SO}_4^{2-})$  modes. The pattern of bands found with the two  $E_g$  bands flanking the  $F_g$  components (Figure 1) is similar to that found for  $\text{CsAl}(\text{SO}_4)_2 \cdot 12\text{H}_2\text{O}$  where weak coupling was observed between the  $\nu_2(\text{AlO}_6)$  and  $\nu_2(\text{SO}_4^{2-})$  modes. The extent of coupling may be estimated from consideration of the additional spectra of  $\text{CsFe}(\text{SO}_4)_2 \cdot 12\text{D}_2\text{O}$  and  $\text{CsFe}(\text{SO}_4)_2 \cdot 12\text{H}_2\text{O}$ .

For  $\text{CsFe}(\text{SO}_4)_2 \cdot 12\text{D}_2\text{O}$  a strong band of  $F_g$  symmetry is found at  $456 \text{ cm}^{-1}$  together with a band of  $E_g$  symmetry at  $464 \text{ cm}^{-1}$ . These bands are assigned to the  $\nu_2(\text{SO}_4^{2-})$  mode on the basis of their intensity and position. Although there are

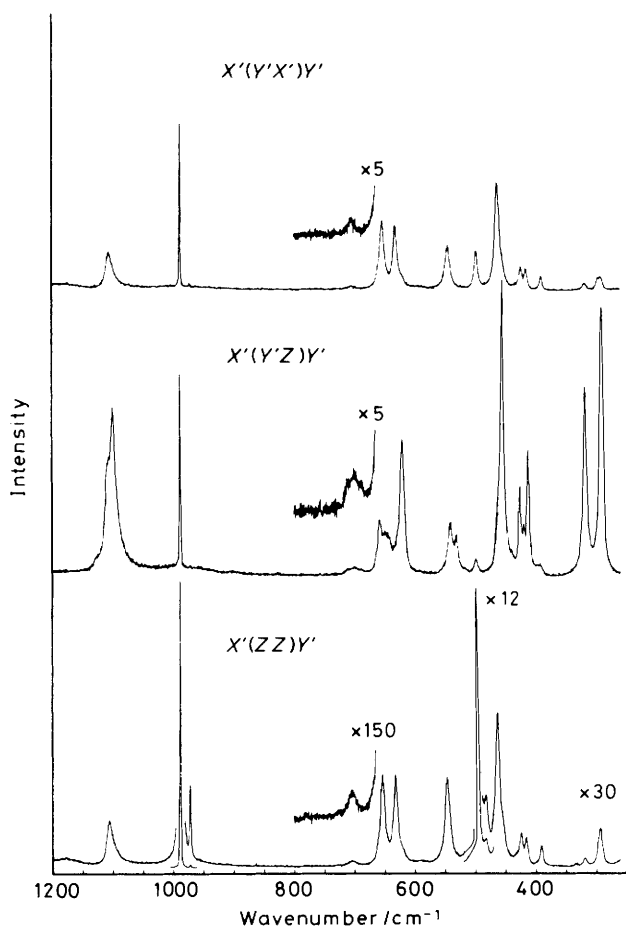


Figure 3. Single-crystal Raman spectra of  $\text{CsFe}(\text{SO}_4)_2 \cdot 12\text{D}_2\text{O}$  at 80 K. Spectral bandwidth  $1.7 \text{ cm}^{-1}$  at  $600 \text{ cm}^{-1}$ ; step size  $0.4 \text{ cm}^{-1}$ ; 50-mW, 487.98-nm radiation at sample. Sensitivities:  $X'(ZZ)Y'$ , 110 180;  $X'(Y'Z)Y'$ , 1 630;  $X'(Y'X')Y'$ , 2 460 counts  $\text{s}^{-1}$

other modes close by, these do not appear to couple strongly with it since there is little apparent intensity borrowing (Figure 3). Irrespective of the extent of coupling the sum of the two  $E_g$  components for the  $\nu_2(\text{FeO}_6)$  and the  $\nu_2(\text{SO}_4^{2-})$  modes of  $\text{CsFe}(\text{SO}_4)_2 \cdot 12\text{H}_2\text{O}$  is constant at  $905 \pm 2 \text{ cm}^{-1}$ . If we assume that the factor-group coupling and force constants remain the same on deuteration and that the  $\nu_2(\text{SO}_4^{2-})$  mode of  $\text{CsFe}(\text{SO}_4)_2 \cdot 12\text{D}_2\text{O}$  is not strongly coupled, then an estimate of the uncoupled frequency for the  $\nu_2(\text{FeO}_6)$  mode of  $\text{CsFe}(\text{SO}_4)_2 \cdot 12\text{H}_2\text{O}$  is  $442 \pm 5 \text{ cm}^{-1}$ . The  $\nu_2(\text{FeO}_6)$  mode is expected to shift on deuteration with the ratio  $\nu_D/\nu_H$  of 0.95, that is to  $420 \pm 3 \text{ cm}^{-1}$ . Bands of  $E_g$  symmetry are found at 424 and  $417 \text{ cm}^{-1}$ . The shift on deuteration is in equally good agreement with either band. However, an external mode found at  $573 \text{ cm}^{-1}$  for  $\text{CsFe}(\text{SO}_4)_2 \cdot 12\text{H}_2\text{O}$  is expected to shift with the ratio  $\nu_D/\nu_H$  of 0.723, that is to  $418 \text{ cm}^{-1}$  in close agreement with the band found at  $417 \text{ cm}^{-1}$ . Hence the band at  $424 \text{ cm}^{-1}$  is predominantly of  $\nu_2(\text{FeO}_6)$  character. Some coupling between these modes is likely because the band of predominantly  $\nu_2(\text{FeO}_6)$  character is found somewhat higher in energy and the component arising from an external mode is found somewhat lower in energy than calculated. This pattern of bands is typical of the presence of coupling. The  $F_g$  components are found at 427, 421, and  $414 \text{ cm}^{-1}$ . The assignment of these bands to either the  $\nu_2(\text{FeO}_6)$  or the external mode is made on the basis of the shifts found on deuteration. The band found

at  $414 \text{ cm}^{-1}$  must be assigned to a component of the external mode since its position is consistent with the shift calculated for the band found at  $572 \text{ cm}^{-1}$  for  $\text{CsFe}(\text{SO}_4)_2 \cdot 12\text{H}_2\text{O}$  ( $\nu_D/\nu_H = 0.723$ ) and it is inconsistent with the calculated position for  $\nu_2(\text{FeO}_6)$  of  $420 \text{ cm}^{-1}$ . The other  $F_g$  component of the external mode in  $\text{CsFe}(\text{SO}_4)_2 \cdot 12\text{H}_2\text{O}$  is found at  $585 \text{ cm}^{-1}$ . The expected position of this band in the deuterate,  $427 \text{ cm}^{-1}$ , is in excellent agreement with the band found at  $427 \text{ cm}^{-1}$ . The remaining  $F_g$  component found at  $421 \text{ cm}^{-1}$  is assigned to the  $\nu_2(\text{FeO}_6)$  mode since it is close to the observed  $E_g$  component and in excellent agreement with the calculated value ( $420 \pm 3 \text{ cm}^{-1}$ ). The extent of coupling is difficult to determine since the intensities and to a lesser extent the energies of the external modes may change on deuteration as a consequence of small changes in the force field. Since the  $E_g$  components of these modes couple there is the likelihood of similar coupling between the  $F_g$  components.

For  $\text{CsFe}(\text{SeO}_4)_2 \cdot 12\text{H}_2\text{O}$ , bands of  $E_g$  symmetry are found at 415, 474, and  $511 \text{ cm}^{-1}$ . Spectra of aluminium selenate alums<sup>2,13</sup> and of alkaline-earth-metal selenates<sup>20</sup> indicate that the  $\nu_4(\text{SeO}_4^{2-})$  mode should be found between 404 and  $440 \text{ cm}^{-1}$ . The bands found at 415 ( $E_g + F_g$ ) and  $433 \text{ cm}^{-1}$  ( $F_g$ ) are assigned to this mode on account of their position and their relative intensities (Figure 2). This leaves the bands at 474 and  $511 \text{ cm}^{-1}$  as the only contenders for the  $\nu_2(\text{FeO}_6)$  mode. The internal modes of the iron(III) hexa-aqua-cation are expected to be insensitive to substitution of selenate for sulphate. The  $\nu_1(\text{FeO}_6)$  mode is found at the same wavenumber for both  $\text{CsFe}(\text{SO}_4)_2 \cdot 12\text{H}_2\text{O}$  and  $\text{CsFe}(\text{SeO}_4)_2 \cdot 12\text{H}_2\text{O}$  and the uncoupled  $\nu_2(\text{AlO}_6)$  mode of  $\text{CsAl}(\text{SO}_4)_2 \cdot 12\text{H}_2\text{O}$  shifts by only  $9 \pm 5 \text{ cm}^{-1}$  to higher energy in  $\text{CsAl}(\text{SeO}_4)_2 \cdot 12\text{H}_2\text{O}$ . Since the uncoupled  $\nu_2(\text{FeO}_6)$  mode occurs at  $442 \pm 5 \text{ cm}^{-1}$  in  $\text{CsFe}(\text{SO}_4)_2 \cdot 12\text{H}_2\text{O}$ , only the bands found at 474 ( $E_g$ ) and  $471 \text{ cm}^{-1}$  ( $F_g$ ) for  $\text{CsFe}(\text{SeO}_4)_2 \cdot 12\text{H}_2\text{O}$  remain as candidates for the  $\nu_2(\text{FeO}_6)$  mode. The bands found at 493 ( $A_g$ ), 511 ( $E_g$ ), and  $517 \text{ cm}^{-1}$  ( $F_g$ ) are assigned to an external mode of co-ordinated water. Although the  $\nu_1(\text{AlO}_6)$  mode is found 19  $\text{cm}^{-1}$  to higher energy than the  $\nu_1(\text{FeO}_6)$  mode, the  $\nu_2(\text{AlO}_6)$  mode is found at  $473 \text{ cm}^{-1}$  in  $\text{CsAl}(\text{SeO}_4)_2 \cdot 12\text{H}_2\text{O}$ , that is, at the same wavenumber as the  $\nu_2(\text{FeO}_6)$  mode. The relatively large shift found for the  $\nu_2(\text{FeO}_6)$  mode ( $32 \text{ cm}^{-1}$ ) on substitution of selenate for sulphate suggests the presence of coupling with another mode of which the  $\nu_4(\text{SeO}_4^{2-})$  mode is the likely partner.

$\nu_5(\text{FeO}_6)$ . The lowest-energy set of bands found for  $\text{CsFe}(\text{SO}_4)_2 \cdot 12\text{H}_2\text{O}$  occurs at 312 ( $E_g$ ) and 306 and  $332 \text{ cm}^{-1}$  ( $F_g$ ). The assignment of this group to the remaining Raman-active internal mode of the  $[\text{Fe}(\text{OH}_2)_6]^{3+}$  octahedral species is established by the shift observed on deuteration for which  $\nu_D/\nu_H = 0.96 \pm 0.01$ , in agreement with the expected ratio of 0.943. The f.g.a. prediction for the  $\nu_5(\text{FeO}_6)$  mode is  $A_g + E_g + 3F_g$  bands. The  $A_g$  component is too weak to be observed in  $\text{CsFe}(\text{SO}_4)_2 \cdot 12\text{H}_2\text{O}$  but is found in  $\text{CsFe}(\text{SO}_4)_2 \cdot 12\text{D}_2\text{O}$ . The missing  $F_g$  component is either weak or accidentally degenerate with either of the  $F_g$  components observed. For both these atoms there are no other bands between 275 and  $400 \text{ cm}^{-1}$  (Figures 1 and 3). Consequently there is no observable coupling between this mode and other allowed modes. The relative intensities and relative band positions are similar for both these alums (Figures 1 and 3) and also for the respective aluminium alums<sup>2</sup> where the  $\nu_5(\text{AlO}_6)$  mode was found at ca. 363 ( $A_g$ ), 343 ( $E_g$ ), and 340 and  $359 \text{ cm}^{-1}$  ( $F_g$ ). The wavenumber shifts reflect the relative strengths of the aluminium- and iron(III)-water bonds. The similarity of the spectra indicates that coupling with other modes is absent and that the sites occupied by both the aluminium and the iron(III) hexa-aqua-cations are similar, the site splitting and factor-group coupling being nearly identical.

**Table 2.** Vibrational frequencies and assignments for  $\text{CsFe}(\text{SO}_4)_2 \cdot 12\text{H}_2\text{O}$ , between 275 and 1 200  $\text{cm}^{-1}$ 

$\bar{\nu}/\text{cm}^{-1}$		$Z(Y'Y')X'$	$Z(X'Z)X'$	$Z(X'Y')X'$	Assignment
306	$F_g$	170	170	16	} $\nu_3(\text{FeO}_6)$
312	$E_g$			4	
332	$F_g$	107	107	12	
432	$E_g$			41	} $\nu_2(\text{SO}_4^{2-})$ + $\nu_2(\text{FeO}_6)$
436	$F_g$	83	85		
445	$F_g$	15	20	5	
460	$F_g$	95	100	3	
473	$E_g$	8	3	50	
523	$A_g$	680	8	25	$\nu_1(\text{FeO}_6)$
540	$F_g$	20	28		} $\rho_6$
542	$E_g + F_g (?)$		sh	32	
572	$F_g$	33	15		} $\rho_5$
573	$E_g$			106	
585	$F_g$	8	8		
608	$F_g$	46	58	3	} $\nu_4(\text{SO}_4^{2-})$
628	$F_g$	85	85		
630	$E_g$			107	} $\rho_4$
664	$A_g$	2.5			
678	$F_g$	8	2		
679	$E_g$			33	
701	$F_g$	2	3		
721	$F_g$	7	10		} $\rho_3$
742	$F_g$	18	7		
746	$E_g$			16	} [573 ( $E_g$ ) + 190 ( $E_g$ )]
764	$E_g$			2	
866	$A_g$	7			
882	$E_g$			7	} $\rho_2$
885	$F_g$	5	5		
954	$F_g$		1.5		} $\rho_1$
955	$E_g$			10	
961	$A_g$	20			$\nu_1(\text{S}^{16}\text{O}_3^{18}\text{O}^{2-})$ $\nu_1(\text{SO}_4^{2-})$
972	$A_g$	30			
988	$A_g$	3 430	109	109	} $\nu_2(\text{SO}_4^{2-})$
1 087	$F_g$	98	112		
1 095	$E_g$			48	
1 097	$F_g$	30	35		} $\nu_2(\text{SO}_4^{2-})$
1 115	$F_g$	5	5		

For  $\text{CsFe}(\text{SeO}_4)_2 \cdot 12\text{H}_2\text{O}$  the spectrum is complicated by the presence of the  $\nu_2(\text{SeO}_4^{2-})$  mode which is expected between 330 and 360  $\text{cm}^{-1}$ .<sup>2,13,20</sup> The bands found at 344 ( $E_g$ ) and 347 and 359  $\text{cm}^{-1}$  ( $F_g$ ) are assigned to the  $\nu_2(\text{SeO}_4^{2-})$  mode on account of their positions and intensities (Figure 2). The remaining bands found at 300 ( $E_g$ ) and 293, 305, and 321  $\text{cm}^{-1}$  ( $F_g$ ) are assigned to the  $\nu_3(\text{FeO}_6)$  mode. Consideration of the relative intensities of the two sets of bands, particularly for the  $E_g$  components (Figure 2), indicates that at most only weak coupling affects the spectrum. This is in contrast to the results for  $\text{CsAl}(\text{SeO}_4)_2 \cdot 12\text{H}_2\text{O}$  where strong coupling between the  $\nu_3(\text{AlO}_6)$  and  $\nu_2(\text{SeO}_4^{2-})$  modes results as a consequence of the former mode lying closer in energy to the selenate mode. The differences between the wavenumbers and bandshapes of the  $\nu_3(\text{FeO}_6)$  mode of  $\text{CsFe}(\text{SO}_4)_2 \cdot 12\text{H}_2\text{O}$  and  $\text{CsFe}(\text{SeO}_4)_2 \cdot 12\text{H}_2\text{O}$  indicate that the sites and/or the field about the sites are substantially different and may reflect the  $\alpha, \beta$  structural change which occurs for the selenate analogues of the caesium sulphate alums.<sup>21</sup>

(ii) *Internal modes of  $\text{SO}_4^{2-}$  and  $\text{SeO}_4^{2-}$ .*  $\nu_1(\text{SO}_4^{2-})$ . The totally symmetric sulphate stretch is found to be very intense and occurs at 989  $\text{cm}^{-1}$  for both  $\text{CsAl}(\text{SO}_4)_2 \cdot 12\text{H}_2\text{O}$  and  $\text{CsAl}(\text{SO}_4)_2 \cdot 12\text{D}_2\text{O}$ . For the corresponding iron(III) alums very strong bands of  $A_g$  symmetry are found at 988  $\text{cm}^{-1}$ . The expected  $F_g$  component in both cases is either vanishingly weak or is coincident with the  $A_g$  component and cannot be distinguished from the leakage of it into the other polarisations. A band of  $A_g$  symmetry arising from the  $\nu_1(\text{S}^{16}\text{O}_3^{18}\text{O}^{2-})$  mode

is expected with a relative intensity of 0.75%. Sharp bands of  $A_g$  symmetry are found at 972.4  $\text{cm}^{-1}$  for both the iron alums with relative intensities of  $0.9 \pm 0.2\%$ .

$\nu_1(\text{SeO}_4^{2-})$ . The assignment of the  $\nu_1(\text{SeO}_4^{2-})$  mode is similarly straightforward with an extremely strong band of  $A_g$  symmetry found at 844  $\text{cm}^{-1}$ . As with the sulphate alums the expected  $F_g$  component is weak and could not be unambiguously separated from the leakage of the strong  $A_g$  component. The results for  $\text{CsFe}(\text{SeO}_4)_2 \cdot 12\text{H}_2\text{O}$  are also in good agreement with those for  $\text{CsAl}(\text{SeO}_4)_2 \cdot 12\text{H}_2\text{O}$  where the  $\nu_1(\text{SeO}_4^{2-})$  mode is found at 845  $\text{cm}^{-1}$ .

$\nu_2(\text{SO}_4^{2-})$  and  $\nu_2(\text{SeO}_4^{2-})$ . The  $\nu_2(\text{SO}_4^{2-})$  mode in  $\text{CsFe}(\text{SO}_4)_2 \cdot 12\text{H}_2\text{O}$  is involved in coupling with the  $\nu_2(\text{FeO}_6)$  mode and has been treated in that context as has the  $\nu_2(\text{SeO}_4^{2-})$  mode which is involved in coupling with the  $\nu_3(\text{FeO}_6)$  mode. For  $\text{CsFe}(\text{SO}_4)_2 \cdot 12\text{D}_2\text{O}$  the  $\nu_2(\text{FeO}_6)$  mode is sufficiently displaced for this coupling to be removed. The bands found at 456 ( $F_g$ ) and 464  $\text{cm}^{-1}$  ( $E_g$ ) are assigned to the  $\nu_2(\text{SO}_4^{2-})$  mode. These results are in close agreement with those obtained from  $\text{CsAl}(\text{SO}_4)_2 \cdot 12\text{D}_2\text{O}$  where the bands are found at 457 ( $F_g$ ) and 465  $\text{cm}^{-1}$  ( $E_g$ ). In both cases the remaining  $F_g$  component is either weak or is coincident with the observed  $F_g$  component. The separation of the  $E_g$  and  $F_g$  components is 8  $\text{cm}^{-1}$  in both cases even though the wavenumber of the close-lying bands is different in the two cases. This splitting must result from factor-group coupling because such a splitting resulting from coupling involving the  $\nu_2(\text{SO}_4^{2-})$  mode would be sensitive to changes in the energies of nearby modes

**Table 3.** Vibrational frequencies and assignments for CsFe(SeO<sub>4</sub>)<sub>2</sub>·12H<sub>2</sub>O, between 275 and 1 200 cm<sup>-1</sup>

$\nu/\text{cm}^{-1}$		$X'(Y'Y')Z$	$X'(ZX')Z$	$X'(Y'X')Z$	Assignment
293	$F_g$	6	6		} $\nu_3(\text{FeO}_6)$
300	$E_g$ (?)			1	
305	$F_g$	43	45	4	
321	$F_g$	9	10		
344	$E_g$			113	} $\nu_2(\text{SeO}_4^{2-})$
347	$F_g$	88	77	4	
359	$F_g$	50	50		} $\nu_4(\text{SeO}_4^{2-})$
415	$E_g + F_g$ (?)	46	3	169	
433	$F_g$	102	114	11	} $\nu_2(\text{FeO}_6)$
471	$F_g$	35	35		
474	$E_g$			29	} $\rho_6$
493	$A_g$	2.5			
511	$E_g$			7	} $\nu_1(\text{FeO}_6)$
517	$F_g$	sh	25		
523	$A_g$	142		4	} $\rho_5$
530	$F_g$		2		
611	$F_g$	8	7		} $\rho_4$
615	$E_g$			9	
623	$A_g$	1.5			} $\rho_3$
702	$E_g$	2	1	9	
710	$A_g$	8		1	} $\rho_2$
720	$F_g$	2	2		
741	$F_g$	6.5	7	1	} $\rho_1$
778	$E_g + F_g$		2.5	5	
787	$A_g$	25		1	} $[787 (A_g) + 36 (A_g)]$ $\nu_1(\text{SeO}_4^{2-})$
823	$A_g$	2			
844	$A_g$	1 700	30	45	} $\rho_2$
851	$F_g$		10		
855	$E_g$			50	} $\nu_3(\text{SeO}_4^{2-})$
860	$A_g$	30			
870	$A_g$	16			} $\nu_3(\text{SeO}_4^{2-})$
872	$F_g$		6		
882	$F_g$	6	6		} $\rho_1$
883	$E_g$			8	
890	$F_g$	166	167	13	} $\rho_1$
935	$F_g$	2	2		
939	$E_g$			3	} $\rho_1$
968	$F_g + A_g$ (?)	6	6		

$\nu_3(\text{SO}_4^{2-})$ . Vibrational studies of alkaline-earth-metal sulphates<sup>18,19</sup> and of alums<sup>2,13</sup> indicate that the  $\nu_3(\text{SO}_4^{2-})$  mode will be found near 1 100 cm<sup>-1</sup>. For CsFe(SO<sub>4</sub>)<sub>2</sub>·12H<sub>2</sub>O the only bands found in the region between 1 000 and 1 200 cm<sup>-1</sup> are at 1 095 ( $E_g$ ) and 1 087, 1 097, and 1 115 cm<sup>-1</sup> ( $F_g$ ). The assignment of these bands to the  $\nu_3(\text{SO}_4^{2-})$  mode is confirmed by the similarity of the bands found in this region for CsFe(SO<sub>4</sub>)<sub>2</sub>·12D<sub>2</sub>O (Figure 3) and their absence in the spectrum of CsFe(SeO<sub>4</sub>)<sub>2</sub>·12H<sub>2</sub>O (Figure 2). The 10-cm<sup>-1</sup> shift to higher energy found on deuteration is consistent with that found for CsAl(SO<sub>4</sub>)<sub>2</sub>·12H<sub>2</sub>O and CsAl(SO<sub>4</sub>)<sub>2</sub>·12D<sub>2</sub>O and is most likely due to small changes in the strength of the hydrogen bonding.

$\nu_3(\text{SeO}_4^{2-})$ . The  $\nu_3(\text{SeO}_4^{2-})$  mode occurs in the region between 850 and 900 cm<sup>-1</sup>.<sup>2,13,20</sup> A complicated spectrum results since external modes of co-ordinated water also occur in this region. Bands are found at 860 and 870 ( $A_g$ ), 855 and 883 cm<sup>-1</sup> ( $E_g$ ), and 851, 872, 882, and 890 cm<sup>-1</sup> ( $F_g$ ). From the count of the number of  $E_g$  bands, only one external mode occurs with the  $\nu_3(\text{SeO}_4^{2-})$  mode. Since the  $\nu_3(\text{SeO}_4^{2-})$  mode is expected to be considerably stronger than the external mode the assignment of the bands should follow from their relative intensities. A strong  $F_g$  component is found at 890 cm<sup>-1</sup> and can then be assigned to the  $\nu_3(\text{SeO}_4^{2-})$  mode. The remaining bands are found to have similar intensities contrary to our expectations. The intensity pattern is consistent with the presence of coupling between the  $\nu_3(\text{SeO}_4^{2-})$  and the external

mode. The further assignment of the bands to uncoupled modes or the quantification of the coupling requires the study of CsFe(SeO<sub>4</sub>)<sub>2</sub>·12D<sub>2</sub>O and is outside the scope of the present work.

$\nu_4(\text{SO}_4^{2-})$  and  $\nu_4(\text{SeO}_4^{2-})$ . The  $\nu_4(\text{SO}_4^{2-})$  mode is found at 630 ( $E_g$ ) and 608 and 628 cm<sup>-1</sup> ( $F_g$ ) for CsFe(SO<sub>4</sub>)<sub>2</sub>·12H<sub>2</sub>O. The absence or presence of similar bands in the spectra of CsFe(SeO<sub>4</sub>)<sub>2</sub>·12H<sub>2</sub>O and CsFe(SO<sub>4</sub>)<sub>2</sub>·12D<sub>2</sub>O (Figures 1—3) enables the assignment of these bands to sulphate vibrations. Comparison with the published spectra of alkaline-earth-metal sulphates<sup>18,19</sup> indicates that they arise from the  $\nu_4(\text{SO}_4^{2-})$  mode. These results are also in good agreement with those for CsAl(SO<sub>4</sub>)<sub>2</sub>·12H<sub>2</sub>O where bands are found at 634 ( $E_g$ ) and 613 and 633 cm<sup>-1</sup> ( $F_g$ ). For CsFe(SO<sub>4</sub>)<sub>2</sub>·12D<sub>2</sub>O an external mode is found nearby and is involved in coupling with the  $\nu_4(\text{SO}_4^{2-})$  mode. This coupling is most clearly seen in the  $E_g$  spectrum where the bands found at 633 and 654 cm<sup>-1</sup> are too intense to be assigned to an external mode which is weak in the hydrate [*cf.* 882 cm<sup>-1</sup> ( $E_g$ ), Figure 1]. This finding is substantiated by the shift found on deuteration for the  $E_g$  component of the external mode which has ratios of  $\nu_D/\nu_H$  which straddle the expected 0.723 for the two bands of CsFe(SO<sub>4</sub>)<sub>2</sub>·12D<sub>2</sub>O (Table 5). The  $F_g$  bands exhibit a more complex pattern. The band at 621 cm<sup>-1</sup> does not appear to be involved in coupling as is demonstrated by its intensity which is similar to that found for CsFe(SO<sub>4</sub>)<sub>2</sub>·12H<sub>2</sub>O. The bands on the high-wavenumber side of that band result from coupling

**Table 4.** Vibrational frequencies and assignments for  $\text{CsFe}(\text{SO}_4)_2 \cdot 12\text{D}_2\text{O}$ , between 275 and 1 200  $\text{cm}^{-1}$ 

$\tilde{\nu}/\text{cm}^{-1}$		$X'(ZZ)Y'$	$X'(Y'Z)Y'$	$X'(Y'X')Y'$	Assignment
292	$F_g$		151	6	} $\nu_5(\text{FeO}_6)$
294	$A_g$	5			
297	$E_g$	5		9	
319	$F_g$		105	4	
391	$E_g$	6		13	
394	$F_g$		4		} $\rho_6$
414	$F_g$		68		
417	$E_g$	8		18	} $\rho_5$ +
421	$F_g$		16		
424	$E_g$	10		20	
427	$F_g$		35		} $\nu_2(\text{FeO}_6)$
430	$A_g + F_g$	2	3		
456	$F_g$		169		} $\nu_2(\text{SO}_4^{2-})$
464	$E_g$	44		87	
483	$A_g$	7			
498	$E_g$			39	} $\rho_4$
500	$A_g$	168	3		
532	$F_g$		11		} $\nu_1(\text{FeO}_6)$
542	$F_g$		20		
545	$E_g$			32	
547	$A_g$	22			} $\rho_3$
621	$F_g$		72		
633	$E_g$	26		54	} $\rho_2$ +
643	$F_g$		10		
649	$F_g$		10		
654	$E_g$	25		53	
659	$F_g$		26		
696	$F_g$		3		} $\nu_4(\text{SO}_4^{2-})$
702	$E_g$			1	
704	$A_g (?)$	1			} $\rho_1$
972	$A_g$	20			
988	$A_g$	2 104	55	167	} $\nu_1(\text{S}^{16}\text{O}_3^{18}\text{O}^{2-})$ $\nu_1(\text{SO}_4^{2-})$
1 100	$F_g$		56		
1 106	$E_g$	8		16	} $\nu_3(\text{SO}_4^{2-})$
1 108	$F_g$		20		
1 127	$F_g$		4		

**Table 5.** The ratio  $\nu_D/\nu_H$  for the external modes of the caesium iron sulphate alums

Assignment	$\text{CsFe}(\text{SO}_4)_2 \cdot 12\text{H}_2\text{O}$	$\nu_D/\nu_H$	$\text{CsFe}(\text{SO}_4)_2 \cdot 12\text{D}_2\text{O}$	
$\rho_6$	542 [ $E_g + F_g (?)$ ]	0.72	391 ( $E_g$ )	} weak coupling with $\nu_2(\text{FeO}_6)$
	540 ( $F_g$ )	0.73	394 ( $F_g$ )	
$\rho_5$	572 ( $F_g$ )	0.72	414 ( $F_g$ )	
	573 ( $E_g$ )	0.73	417 ( $E_g$ )	
	585 ( $F_g$ )	0.73	427 ( $F_g$ )	
	664 ( $A_g$ )	0.73	483 ( $A_g$ )	
$\rho_4$	678 ( $F_g$ )	0.73	498 ( $E_g$ )	
	679 ( $E_g$ )			
	701 ( $F_g$ )			
$\rho_3$	721 ( $F_g$ )	0.74	532 ( $F_g$ )	
	742 ( $F_g$ )	0.73	542 ( $F_g$ )	
	746 ( $E_g$ )	0.73	545 ( $E_g$ )	
	866 ( $A_g$ )	0.74	633 ( $E_g$ )	
882 ( $E_g$ )				
$\rho_2$	885 ( $F_g$ )	0.70	654 ( $E_g$ )	
		0.72	621 ( $F_g$ )	
		0.73	643 ( $F_g$ )	
		0.73	649 ( $F_g$ )	
		0.74	659 ( $F_g$ )	
		0.73	696 ( $F_g$ )	
$\rho_1$	954 ( $F_g$ )	0.74	702 ( $E_g$ )	
	955 ( $E_g$ )	0.74	704 [ $A_g (?)$ ]	
	961 ( $A_g$ )	0.73		

between the other  $F_g$  component of the  $\nu_4(\text{SO}_4^{2-})$  mode and the external mode. This is demonstrated by the shifts on deuteration which are shown in Table 5. The band at 621  $\text{cm}^{-1}$  lies well away from the expected wavenumber of the

external mode with the other three bands straddling the expected ratio of 0.723. The  $\nu_4(\text{SeO}_4^{2-})$  mode was discussed in the relation to the assignment of the  $\nu_2(\text{FeO}_6)$  mode.

(iii) *The external modes of co-ordinated water.* The externa

**Table 6.** Vibrational frequencies and assignments for  $\text{CsCr}(\text{SO}_4)_2 \cdot 12\text{H}_2\text{O}$ , between 275 and 1 200  $\text{cm}^{-1}$ 

$\nu/\text{cm}^{-1}$		$Z(Y'Y')X'$	$Z(X'Y')X'$	$Z(X'Y')X'$	Assignment
312	$F_g$	51	81	15	} $\nu_3(\text{CrO}_6)$
315	$E_g$			1	
336	$F_g$	27	46	8	
448	$F_g$		169	91	} $\nu_2(\text{SO}_4^{2-})$
449	$E_g$	113	46	170	
469	$F_g$	3	9		} [152 ( $F_g$ ) + 318 ( $F_g$ )]
500	$F_g$	4	7		
504	$E_g$			29	} $\nu_2(\text{CrO}_6)$
540	$A_g$	169	15		
541	$E_g$		10	41	} $\nu_1(\text{CrO}_6)$
569	$F_g$		3		
571	$E_g$	5		48	} $\rho_6$
590	$F_g$		1		
607	$F_g$	12	26		} $\nu_4(\text{SO}_4^{2-})$
628	$F_g$	36	58		
629	$E_g$			70	
679	$E_g$	2		21	} $\rho_4$
705	$F_g$		3		
713	$F_g$	5	7		} $\rho_3$
729	$F_g$		3		
739	$A_g$	4			
741	$E_g$			13	} [541 ( $E_g$ ) + 218 ( $E_g$ )]
759	$E_g$			2.5	
881	$A_g$	2			} $\rho_2$
895	$E_g$			5	
899	$F_g$	3	4		} $\rho_1$
959	$E_g$			8	
961	$A_g$	7			} $\nu_1(\text{S}^{16}\text{O}_3^{18}\text{O}^{2-})$
973	$A_g$	14			
988	$A_g$	1 363	103	140	} $\nu_1(\text{SO}_4^{2-})$
1 088	$F_g$	33	68	5	
1 095	$E_g$			17	} $\nu_3(\text{SO}_4^{2-})$
1 096	$F_g$	7	13		
1 111	$F_g$	4	7		

modes of co-ordinated water, the rocks, wags, and twists, will occur for both the monovalent and trivalent hexa-aquations. The relative ordering of these modes is determined by both the nature of the co-ordination and the directional nature of the hydrogen bonding.<sup>2</sup> In the absence of normal-coordinate analysis based on neutron-diffraction data, we will not attempt to assign the bands found to specific external modes, rather the nomenclature adopted for the caesium aluminium alums is most appropriate. The six external modes will be labelled  $\rho_1$ — $\rho_6$  in order of decreasing wavenumber, where  $\rho_1$ — $\rho_3$  are most likely associated with the  $[\text{Fe}\{\text{O}(\text{H},\text{D})_2\}_6]^{3+}$  and  $\rho_4$ — $\rho_6$  with the  $[\text{Cs}\{\text{O}(\text{H},\text{D})_2\}_6]^+$ .

Because each of the external modes has one component of  $E_g$  symmetry and for both  $\text{CsFe}(\text{SeO}_4)_2 \cdot 12\text{H}_2\text{O}$  and  $\text{CsFe}(\text{SO}_4)_2 \cdot 12\text{D}_2\text{O}$  there are six bands of  $E_g$  symmetry to be accounted for, their assignment to the external modes is simply one to one. The  $A_g$  and  $F_g$  components found near their respective  $E_g$  component are assigned accordingly. The complications arising from the coupling of the external modes with internal sulphate or hexa-aquairon(III) modes have already been identified and discussed in the text. For  $\text{CsFe}(\text{SO}_4)_2 \cdot 12\text{H}_2\text{O}$  there are seven bands of  $E_g$  symmetry. The occurrence of greater than the number of bands predicted by the f.g.a. can be explained in terms of the presence of second-order effects or in terms of disorder of the molecular subunits. The assignment of the six external modes can be made by considering the spectrum of  $\text{CsFe}(\text{SO}_4)_2 \cdot 12\text{D}_2\text{O}$  since these modes are expected to shift with the ratio  $\nu_D/\nu_H$  of 0.723. Some deviation from this expected ratio may occur as a result of strong coupling involving external modes; however these deviations have been found to be small. In each case

excellent agreement between the calculated and observed ratios is found (Table 5). The broad weak band of  $E_g$  symmetry found at 764  $\text{cm}^{-1}$  is assigned to the combination of bands of  $E_g$  symmetry found at 573  $\text{cm}^{-1}$ , an external mode, and 190  $\text{cm}^{-1}$ , a low-energy mode involving water. The likelihood that any of the other  $E_g$  components result from second-order effects is discounted because: (i) the ratios  $\nu_D/\nu_H$  found for these bands are in excellent agreement with the expected ratio of 0.723 (Table 5) and bands arising from second-order effects would not exhibit such a shift on deuteration; and (ii) the positions and relative intensities of the external modes of  $\text{CsFe}(\text{SO}_4)_2 \cdot 12\text{H}_2\text{O}$  are in close agreement with those found for  $\text{CsAl}(\text{SO}_4)_2 \cdot 12\text{H}_2\text{O}$ . Once again the  $A_g$  and  $F_g$  components are assigned by making use of the  $E_g$  components.

(B) *Assignment of the Spectra of  $\text{CsCr}(\text{SO}_4)_2 \cdot 12\text{H}_2\text{O}$  and  $\text{CsCr}(\text{SeO}_4)_2 \cdot 12\text{H}_2\text{O}$ .*—The assignments for these spectra are given in Tables 6 and 7, and the spectra are included in SUP 56047. The assignments follow generally from the arguments used above for the spectra of the iron alums and those presented previously for the aluminium alums.<sup>2</sup> For brevity, therefore, only those features which differ significantly will be described.

The  $\nu_1(\text{CrO}_6)$  mode occurs at higher energy than the  $\nu_1(\text{FeO}_6)$  mode and at lower energy than the  $\nu_1(\text{AlO}_6)$  mode, consistent with the Cr—O bond length being intermediate between those of Fe—O and Al—O. Its intensity in the  $A_g$  component is similarly intermediate.

The  $\nu_2(\text{CrO}_6)$  mode occurs at higher wavenumber than the analogous vibrations of the iron and aluminium alums. Consequently it is not coupled with the  $\nu_2(\text{SO}_4^{2-})$  mode as occurs



**Table 7.** Vibrational frequencies and assignments for  $\text{CsCr}(\text{SeO}_4)_2 \cdot 12\text{H}_2\text{O}$ , between 275 and 1 200  $\text{cm}^{-1}$ 

$\nu/\text{cm}^{-1}$		$X'(Y'Y)Z$	$X'(ZY)Z$	$X'(Y'X')Z$	Assignment
297	$F_g$	3	3		} $\nu_3(\text{CrO}_6)$
305	$E_g$			4	
309	$F_g$	21	21		
324	$F_g$	9	9		
347	$E_g$			105	} $\nu_2(\text{SeO}_4^{2-})$
349	$F_g$	70	45		
360	$F_g$	65	75		
416	$F_g$	ca. 3	5		
426	$E_g$	53	ca. 3	169	} $\nu_4(\text{SeO}_4^{2-})$
439	$F_g$	162	163	12	
504	$E_g + F_g$	6	6	5	} $\nu_2(\text{CrO}_6)$
510	$E_g$			15	
515	$F_g$	24	27		} $\rho_6$
525	$F_g$		ca. 1		
540	$A_g + F_g (?)$	73	ca. 2	3	} $\nu_1(\text{CrO}_6)$
610	$F_g$	10	9		
614	$E_g$			12	} $\rho_5$
702	$E_g$	2	1	10	
709	$A_g$	5			} $\rho_4$
718	$F_g$	2	2		
741	$F_g$	5	5		
775	$E_g$	2		7	
783	$F_g$		3		} $\rho_3$
789	$A_g$	8			
845	$A_g$	2 091	45	89	} $\nu_1(\text{SeO}_4^{2-})$
854	$F_g$	ca. 20	11		
857	$E_g$			75	} $\rho_2 +$ $\nu_3(\text{SeO}_4^{2-})$
882	$F_g$	104	113	5	
892	$E_g$			6	} $\rho_1$
936	$F_g$	7	5		
940	$E_g$			11	
975	$F_g$	4	4		

in the iron and aluminium spectra. The assignment of the  $\nu_2(\text{CrO}_6)$  mode of the sulphate alum is confirmed by its similar energy in the selenate alum.

After assignment of the internal modes of  $\text{CrO}_6$  and sulphate or selenate, there remain seven unassigned  $E_g$  bands. Six external modes of co-ordinated water are expected; hence at least one of these bands is due to a second-order effect. A weak band at 759  $\text{cm}^{-1}$  is tentatively assigned to a combination of an external mode (541  $\text{cm}^{-1}$ ) and a low-frequency mode (218  $\text{cm}^{-1}$ ). A similar feature is found in the spectrum of  $\text{CsFe}(\text{SO}_4)_2 \cdot 12\text{H}_2\text{O}$ . In the spectrum of  $\text{CsCr}(\text{SeO}_4)_2 \cdot 12\text{H}_2\text{O}$  only six  $E_g$  bands occur and are assigned to the external modes.

(C) *Assignment of the Spectra of  $\text{CsGa}(\text{SO}_4)_2 \cdot 12\text{H}_2\text{O}$ ,  $\text{CsIn}(\text{SO}_4)_2 \cdot 12\text{H}_2\text{O}$ , and  $\text{CsV}(\text{SO}_4)_2 \cdot 12\text{H}_2\text{O}$ .*—The spectra of these compounds are similar (see SUP 56047) and the assignments are given in Tables 8–10. A strong band of  $A_g$  symmetry can be identified unambiguously as the  $\nu_1(\text{MO}_6)$  totally symmetric metal–ligand stretching mode. For  $\text{CsIn}(\text{SO}_4)_2 \cdot 12\text{H}_2\text{O}$  the strong  $A_g$  component of the  $\nu_1(\text{InO}_6)$  mode found at 505  $\text{cm}^{-1}$  is well away from any other modes, and there is no  $F_g$  intensity above the leakage of the strong  $A_g$  component into the  $F_g$  spectrum. The situation is more complex for the gallium and vanadium atoms, where their respective  $\nu_1(\text{MO}_6)$  modes are found close to bands of  $E_g$  and  $F_g$  symmetry. The bands of  $E_g$  symmetry mark the presence of external modes. The constancy of both the bandshapes and the intensities of the  $F_g$  components suggests that they result from external modes and are not components of the  $\nu_1(\text{MO}_6)$  mode. In all three cases there are no other bands of appreciable  $A_g$  intensity close to the  $\nu_1(\text{MO}_6)$  mode; it follows that in each case the extent of coupling between  $\nu_1(\text{MO}_6)$  and the other modes is small.

The spectra of the three alums are similar in the region between 400 and 500  $\text{cm}^{-1}$ . Strong bands of  $E_g$  and  $F_g$  symmetry are found and in each case the  $E_g$  bands flank the strong  $F_g$  components. Such a pattern of bands is found for the corresponding aluminium and iron alums and is explained in terms of coupling between the  $\nu_2(\text{MO}_6)$  and  $\nu_2(\text{SO}_4^{2-})$  modes. The wavenumbers and relative intensities of the bands are found to change in each case. Both the wavenumber of the  $\nu_2(\text{MO}_6)$  mode and the extent of coupling are metal sensitive. The intensity of the uncoupled  $\nu_2(\text{MO}_6)$  mode will also change with the metal and consequently the interpretation of the spectra will be complex. We can simplify the interpretation by considering the  $E_g$  spectrum because only two bands are expected in this region and these are found for all the caesium alums studied. If we neglect the influence of other modes then for a given caesium alum the sum of the  $E_g$  components of the  $\nu_2(\text{MO}_6)$  and  $\nu_2(\text{SO}_4^{2-})$  modes is constrained to be constant. Since the other internal sulphate modes are insensitive to changing the trivalent metal cation in the caesium  $\beta$ -alums, we will assume that the wavenumber of the uncoupled  $\nu_2(\text{SO}_4^{2-})$  mode remains constant. An estimate of the wavenumber of the latter mode can be obtained from the spectrum of  $\text{CsCr}(\text{SO}_4)_2 \cdot 12\text{H}_2\text{O}$  where the coupling between the  $\nu_2(\text{CrO}_6)$  and  $\nu_2(\text{SO}_4^{2-})$  modes is small. Uncoupled wavenumbers for the  $\nu_2(\text{MO}_6)$  mode can be obtained simply by subtracting the uncoupled  $\nu_2(\text{SO}_4^{2-})$  wavenumber from the sum of the  $E_g$  components of the coupled  $\nu_2(\text{MO}_6)$  and  $\nu_2(\text{SO}_4^{2-})$  modes. For gallium, indium, and vanadium uncoupled wavenumbers for the  $\nu_2(\text{MO}_6)$  mode are calculated to be 450, 444, and 454  $\text{cm}^{-1}$  respectively.

The external modes of co-ordinated water are assigned in the same manner as was outlined for  $\text{CsCr}(\text{SO}_4)_2 \cdot 12\text{H}_2\text{O}$ . There are seven bands of  $E_g$  symmetry to be assigned for the

**Table 8.** Vibrational frequencies and assignments for CsGa(SO<sub>4</sub>)<sub>2</sub>·12H<sub>2</sub>O, between 275 and 1 200 cm<sup>-1</sup>

$\bar{\nu}/\text{cm}^{-1}$		$X'(Y'Y')Z$	$X'(ZX')Z$	$X'(Y'X')Z$	Assignment
318	$F_g$	35	69		} $\nu_3(\text{GaO}_6)$
322	$E_g$			2	
342	$F_g$	19	37	0.5	
429	$E_g$	sh		21	} $\nu_2(\text{SO}_4^{2-})$ + $\nu_2(\text{GaO}_6)$
434	$F_g$	35	73		
458	$F_g$	75	160	2	
470	$E_g$	sh		21	} $\nu_1(\text{GaO}_6)$
537	$A_g$	106			
538	$F_g$		29		} $\rho_6$
540	$E_g$			9	
571	$E_g$			19	} $\rho_5$
572	$F_g$	14	9		
584	$F_g$	6	11		} $\nu_4(\text{SO}_4^{2-})$
608	$F_g$	34	68	0.5	
629	$F_g$	53	92		
630	$E_g$			21	} $\rho_4$
679	$E_g$	5		8	
702	$F_g$		2		} $\rho_3$
716	$A_g + F_g$	3	6		
725	$F_g$	2	4		} [571 ( $E_g$ ) + 194 ( $E_g$ )]
743	$E_g$	7		5	
763	$E_g$				} $\rho_2$
880	$A_g$	2.5			
898	$E_g$	sh		1	} $\rho_1$
905	$F_g$	5	13		
957	$E_g$			3	} $\nu_1(\text{S}^{16}\text{O}_3^{18}\text{O}^{2-})$ $\nu_1(\text{SO}_4^{2-})$
959	$A_g$	7			
974	$A_g$	9			} $\nu_3(\text{SO}_4^{2-})$
989	$A_g$	2 730	136	78	
1 088	$F_g$	47	120		} $\nu_3(\text{SO}_4^{2-})$
1 098	$E_g$			5	
1 100	$F_g$	5	8		
1 115	$F_g$	4	8		

gallium and indium and six for the vanadium alum. In all three cases a weak feature is found close to 760 cm<sup>-1</sup> in the  $E_g$  spectrum. For CsM(SO<sub>4</sub>)<sub>2</sub>·12H<sub>2</sub>O (M = Fe or Cr) similar features are found and are attributable to combination bands. This assignment is made for the gallium, indium, and vanadium caesium alums because the combination of an external mode and a low-frequency mode involving water co-ordinated to the monovalent cation yields a result close in wavenumber to the bands found in each case. The assignment of the external modes for the gallium and indium alums is straightforward because there are six external modes and six bands of  $E_g$  symmetry to be accounted for. The assignment is then one to one with the close-lying  $A_g$  and  $F_g$  components treated accordingly.

In the spectrum of CsV(SO<sub>4</sub>)<sub>2</sub>·12H<sub>2</sub>O only five of the six  $E_g$  bands to be assigned to the external modes are found. A band of  $A_g$  symmetry is found at 958 cm<sup>-1</sup> and on account of its intensity and bandshape can only be assigned to an external mode. The nearest  $E_g$  band is found at 883 cm<sup>-1</sup> and this already has a band of  $A_g$  symmetry close by. The  $E_g$  component in the region of 958 cm<sup>-1</sup> is therefore vanishingly weak. Since this is the highest-energy external mode it is assigned to  $\rho_1$ . The five bands of  $E_g$  symmetry are assigned to the remaining five external modes. The remaining  $A_g$  and  $F_g$  components are treated accordingly. The energies of the six external modes found are in agreement with those found for the other caesium  $\beta$ -alums.

(D) Assignment of the Spectrum of CsTi(SO<sub>4</sub>)<sub>2</sub>·12H<sub>2</sub>O.—Despite the presence of low-wavenumber bands indicative of

the onset of a phase transition, the spectrum of this alum is otherwise similar to those already discussed (see Figure 4 and Table 11). The strong band of  $A_g$  symmetry found at 517 cm<sup>-1</sup> is assigned to the  $\nu_1(\text{TiO}_6)$  mode. Since there are no other bands with appreciable  $A_g$  intensity close by the extent of coupling between the  $\nu_1(\text{TiO}_6)$  and other modes is small.

The pattern of bands found between 400 and 500 cm<sup>-1</sup> is similar to that found for the alums of Ga, In, V, and Fe where there is coupling between the  $\nu_2(\text{MO}_6)$  and  $\nu_2(\text{SO}_4^{2-})$  modes. From this spectrum the wavenumber of the uncoupled  $\nu_2(\text{TiO}_6)$  mode is estimated to be 459 cm<sup>-1</sup>, calculated in the same manner as outlined for the alums of Ga, In, and V. The  $\nu_3(\text{TiO}_6)$  mode is found between 291 and 346 cm<sup>-1</sup>. The relative intensities and the f.w.h.h. of the bands are different from those found for the other caesium  $\beta$ -alums. Since this mode is found well away from other modes it is unlikely that these differences arise from coupling between them.

The internal sulphate modes are found close in wavenumber and with similar intensities to those of the other caesium alums already discussed. The internal sulphate bending modes [ $\nu_2(\text{SO}_4^{2-})$  and  $\nu_4(\text{SO}_4^{2-})$ ] exhibit some broadening while the internal sulphate stretching modes [ $\nu_1(\text{SO}_4^{2-})$  and  $\nu_3(\text{SO}_4^{2-})$ ] remain essentially unchanged.

The external modes of co-ordinated water are assigned by comparison with the spectra of other caesium  $\beta$ -alums. A number of them exhibit considerable broadening. Since the external modes will be most sensitive to structural perturbations the assignments of these bands are tentative. Spectra and structural information obtained at temperatures below that of the phase transition are necessary to analyse unambiguously these modes.

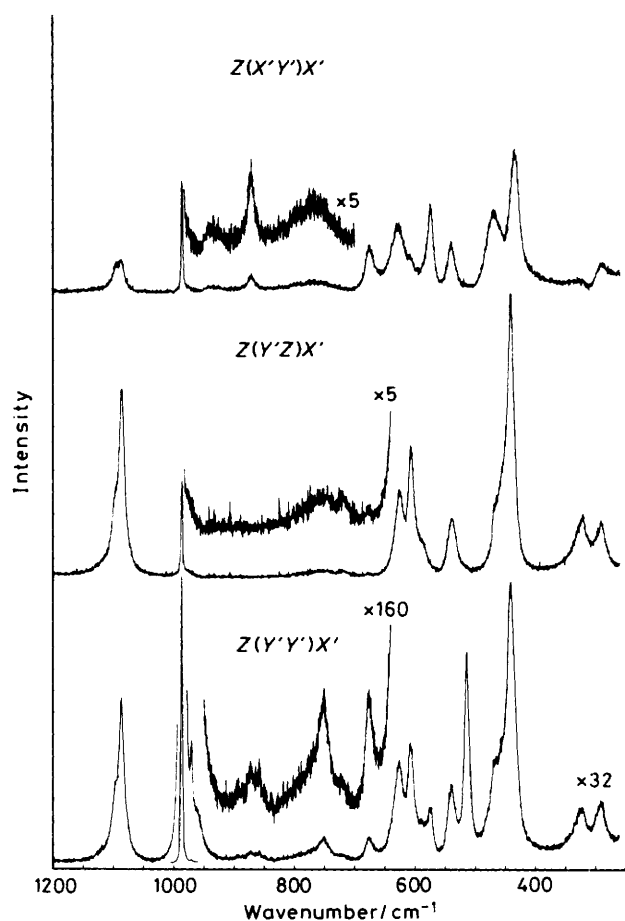


Figure 4. Single-crystal Raman spectra of  $\text{CsTi}(\text{SO}_4)_2 \cdot 12\text{H}_2\text{O}$  at 80 K. Spectral bandwidth  $2.7 \text{ cm}^{-1}$  at  $600 \text{ cm}^{-1}$ ; step size  $0.4 \text{ cm}^{-1}$ ; 70-mW, 647.1-nm radiation at sample. Sensitivities:  $Z(Y'Y')X'$ , 36 450;  $Z(Y'Z)X'$ , 1 061;  $Z(X'Y')X'$ , 936 counts  $\text{s}^{-1}$

### Conclusions

The spectra of the caesium  $\beta$ -alums are found to be similar for a wide variety of trivalent metal cations. The assignment of the Raman-active internal modes of the trivalent hexa-aqua-cation has been established by isotope and anion substitution. These modes exhibit both a wavenumber and an intensity dependence on the identity of the metal. The internal sulphate modes and the external modes of co-ordinated water are insensitive to changing the trivalent metal cation which implies that the lattice and the force field about this species remain essentially constant. It follows that, in the absence of coupling, wavenumber shifts and changes of the intensities of the internal modes of the trivalent hexa-aqua-cation can be attributed to changes in internal force constants and molecular and electronic structure.

The totally symmetric stretching mode provides the simplest means of measuring the metal(III)-water force constant because the wavenumber of this mode is independent of the mass of the metal. The bands arising from this mode are easily identified because they occur as bands of  $A_g$  symmetry that are usually many times more intense than the other  $A_g$  bands in that region of the spectrum. Analysis of the spectra, based on the intensities of these bands, has shown that the extent of coupling between the  $\nu_1(\text{MO}_6)$  and other modes is small. A simple relationship is found between the wavenumber of the  $\nu_1(\text{MO}_6)$  mode and the reciprocal of the

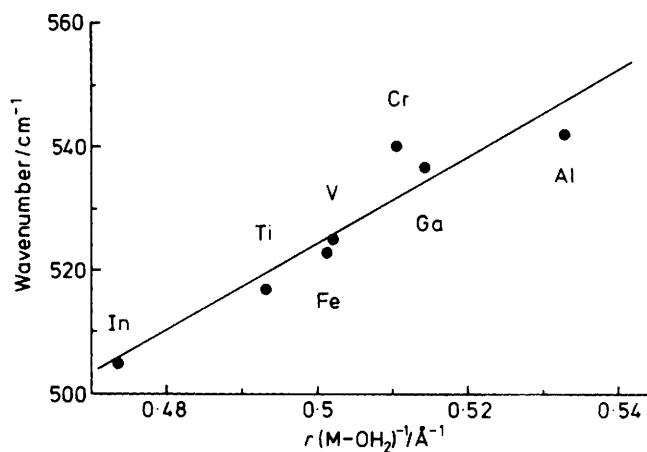


Figure 5. The wavenumber of the totally symmetric stretching mode plotted against the reciprocal of the metal(III)-water bond length. The bond lengths were obtained from ref. 1

metal(III)-water bond length (Figure 5). This relationship is found to be the same for the trivalent hexa-aqua-cations of the first-row transition metals studied and for the Group 3 metals.

The intensities of the  $\nu_1(\text{MO}_6)$  modes are found to be metal sensitive and to change over two orders of magnitude. The  $A_g$  component of the  $\nu_1(\text{FeO}_6)$  mode occurs with most intensity, and the  $A_g$  component of the  $\nu_1(\text{AlO}_6)$  mode is found to be the weakest reported for the caesium sulphate alums. The reasons for the variations of the intensity of  $\nu_1(\text{MO}_6)$  Raman bands are complex; however it is recognised that the covalency of the metal-water bond is an important factor in the intensity of the stretching mode.<sup>9</sup> These variations in the intensities of the  $\nu_1(\text{MO}_6)$  modes do not lead to significant deviations in the relationship between the bond length and the wavenumber of the totally symmetric stretching mode. Consequently, either these differences are not indicative of changes in the covalency of the metal(III)-water bond, or the covalency indicated by the intensity variations is only a small perturbation on the metal(III)-water bond, or the relationship between the bond length and the bond strength is the same for these covalent interactions as for the electrostatic potential.

The wavenumbers of the internal modes of the trivalent hexa-aqua-cation will be perturbed by changes in the strength of the field about it. The magnitude of these effects is unknown. For this species the field will be mediated through hydrogen bonding involving the water molecules co-ordinated to the trivalent cation. The wavenumbers of the external modes of these water molecules are sensitive to hydrogen bonding and consequently are sensitive to the field about the trivalent hexa-aqua-cation.

The external modes of water co-ordinated to the aluminium(III) cation occur about  $100 \text{ cm}^{-1}$  lower in wavenumber for  $[\text{Al}(\text{OH}_2)_6]\text{Cl}_3$  at 115 K<sup>12</sup> than for the caesium alums at 80 K.<sup>2</sup> This indicates that the field about the aluminium(III) hexa-aqua-cation is considerably stronger in the alums than in aluminium chloride. Consistent with this, the  $\nu_1(\text{AlO}_6)$  mode of aluminium chloride occurs at  $524 \text{ cm}^{-1}$ ,  $18 \text{ cm}^{-1}$  to lower wavenumber than for the alums.

The temperature dependence of the  $\nu_1(\text{MO}_6)$  mode in strongly hydrogen-bonded crystals is another example of this outer-sphere effect on the wavenumber of the internal modes of the trivalent hexa-aqua-cation. The increase in the wavenumber of the  $\nu_1(\text{MO}_6)$  mode with decreasing temperature results from an ordering and strengthening of the hydrogen bonding which is reflected by a reduction in the volume of the

**Table 9.** Vibrational frequencies and assignments for CsIn(SO<sub>4</sub>)<sub>2</sub>·12H<sub>2</sub>O, between 275 and 1 200 cm<sup>-1</sup>

$\tilde{\nu}/\text{cm}^{-1}$		$X'(ZZ)Y'$	$X'(Y'Z)Y'$	$X'(Y'X')Y'$	Assignment
291	$F_g$	2	62	6	} $\nu_3(\text{InO}_6)$
297	$E_g$			2.5	
298	$F_g$		4		
300	$A_g(?)$	2			
322	$F_g$	1	35.5	3	
425	$E_g$	31		91	} $\nu_2(\text{SO}_4^{2-})$
430	$F_g$		46		
458	$F_g$	5	169	8	} + $\nu_2(\text{InO}_6)$
468	$E_g$	55		167	
476	$F_g$		3		} $\nu_1(\text{InO}_6)$
505	$A_g$	167	2.5	7	
538	$E_g + F_g$	12	15	42	
544	$F_g$		10		} $\rho_6$
560	$A_g$	3	2		
567	$E_g$	26		77	} $\rho_5$
579	$F_g$		7		
603	$F_g$	2	42	2	} $\nu_4(\text{SO}_4^{2-})$
615	$F_g$		8		
624	$E_g$	41		120	
626	$F_g$		65		
673	$E_g$	24		72	
716	$F_g$		2.5		} $\rho_4$
740	$E_g$			25	
742	$A_g(?)$	12			} $\rho_3$
746	$E_g$			16	
756	$E_g$			2	} [567 ( $E_g$ ) + 203 ( $E_g$ )]
882	$A_g$	3			
893	$E_g$	4		7	} $\rho_2$
898	$F_g$		1		
916	$F_g$		1		
938	$E_g + F_g$		1	18	} $\rho_1$
939	$A_g$	10			
972	$A_g$	19			} $\nu_1(\text{S}^{16}\text{O}_3^{18}\text{O}^{2-})$
988	$A_g$	2 907	39	156	
1 088	$F_g$	2	83		} $\nu_3(\text{SO}_4^{2-})$
1 094	$E_g$	10		27	
1 096	$F_g$		8		
1 106	$F_g$		8		

unit cell. The extent of this effect can be estimated for CsGa(SO<sub>4</sub>)<sub>2</sub>·12H<sub>2</sub>O from a shift of 10 cm<sup>-1</sup> to higher wavenumber on cooling the crystal from 297 to 80 K. However, for the weakly hydrogen-bonded [Ni(OH<sub>2</sub>)<sub>6</sub>]SiF<sub>6</sub> crystal the wavenumber of the  $\nu_1(\text{NiO}_6)$  mode was not observed to change on cooling from 300 to 15 K.<sup>22</sup> The weakness of the field about the nickel(II) hexa-aqua-cation is reflected by the wavenumbers of the external modes of water which are 200 cm<sup>-1</sup> lower in energy than the corresponding modes of the alums.

These observations indicate that the wavenumber of the internal modes of the trivalent hexa-aqua-cation are perturbed by the surrounding field. For the  $\nu_1(\text{MO}_6)$  mode this perturbation may be as large as 20 cm<sup>-1</sup> out of 542 cm<sup>-1</sup> between a strongly and a weakly hydrogen-bonded environment.

The  $\nu_1(\text{MO}_6)$  modes observed for the alum crystals can now be compared with those obtained from solution. The interpretation of these measurements is very often complicated by inner-sphere co-ordination of anions to substitution-labile trivalent cations. The [Cr(OH<sub>2</sub>)<sub>6</sub>]<sup>3+</sup> cation, unlike the other trivalent hexa-aqua-cations studied, is known to be kinetically inert to substitution<sup>23</sup> so for the time-scale of these measurements these problems are not significant. Consequently the analysis of the [Cr(OH<sub>2</sub>)<sub>6</sub>]<sup>3+</sup> cation in aqueous solution is greatly simplified.

In solution a polarised band is reported to occur at 500 cm<sup>-1</sup> for the hydrated chromium(III) species and was assigned to

the  $\nu_1[\text{Cr}(\text{OH}_2)_6^{3+}]$  mode.<sup>10</sup> Solution studies of KCr(SO<sub>4</sub>)<sub>2</sub>·12H<sub>2</sub>O in various concentrations of sulphuric acid carried out in this laboratory indicate that the reported band is sensitive to pH and is found between 490 and 522 cm<sup>-1</sup>. The observed pH dependence is likely to result from the presence of varying concentrations of aquahydroxochromium cations. The observed bands are broad with f.w.h.s of about 40 cm<sup>-1</sup>; we were unable to resolve these features into their different component bands. In sulphuric acid (1 mol dm<sup>-3</sup>) virtually all the aquated chromium(III) will be present as the [Cr(OH<sub>2</sub>)<sub>6</sub>]<sup>3+</sup> cation. Under these conditions a polarised band is found at 522 cm<sup>-1</sup> and assigned to the  $\nu_1[\text{Cr}(\text{OH}_2)_6^{3+}]$  mode. The polarised band reported at 500 cm<sup>-1</sup> is probably due to the presence of aquahydroxochromium cations. In solution the  $\nu_1[\text{Cr}(\text{OH}_2)_6^{3+}]$  mode occurs 18 cm<sup>-1</sup> lower in energy than it does for CsCr(SO<sub>4</sub>)<sub>2</sub>·12H<sub>2</sub>O at 80 K. For the trivalent hexa-aqua-aluminium cation a difference of 17 cm<sup>-1</sup> has been found between the solution measurements<sup>8</sup> and the value obtained through a study of CsAl(SO<sub>4</sub>)<sub>2</sub>·12H<sub>2</sub>O at 80 K.<sup>2</sup> The similarity of these results for aluminium and chromium indicates the transferability of the single-crystal results to the solution state, with a correction of 15–20 cm<sup>-1</sup> due to temperature and medium effects.

For the alums the totally symmetric stretching modes of the trivalent hexa-aqua-cations have been identified unambiguously between 500 and 550 cm<sup>-1</sup>. Previously these cation-water stretching frequencies have been quoted to lie between

**Table 10.** Vibrational frequencies and assignments for CsV(SO<sub>4</sub>)<sub>2</sub>·12H<sub>2</sub>O, between 275 and 1 200 cm<sup>-1</sup>

$\bar{\nu}/\text{cm}^{-1}$		$X'(ZZ)Y'$	$X'(ZX')Y'$	$X'(Y'X')Y'$	Assignment
304	$F_g$		130		} $\nu_3(\text{VO}_6)$
308	$E_g$	17		17	
329	$F_g$	3	78	3	
430	$E_g$	167		167	} $\nu_2(\text{SO}_4^{2-})$ + $\nu_2(\text{VO}_6)$
435	$F_g$		100		
464	$F_g$		123		
472	$E_g$	64		64	} $\nu_1(\text{VO}_6)$
525	$A_g$	95	15	3	
538	$F_g$		30		} $\rho_6$
539	$E_g$	12		12	
570	$F_g$		13		} $\rho_5$
572	$E_g$	35		33	
609	$F_g$	3	85	2	} $\nu_4(\text{SO}_4^{2-})$
626	$F_g$		75		
628	$E_g$	40		40	
677	$E_g$	4		5	} $\rho_4$
726	$F_g$		9		
744	$F_g$		15		} $\rho_3$
746	$E_g$	40		40	
761	$E_g$	1		2	} [572 ( $E_g$ ) + 189 ( $E_g$ )]
866	$A_g$	3			
883	$E_g$	10		10	} $\rho_2$
888	$F_g$		5		
958	$A_g$	8			} $\rho_1$
972	$A_g$	23			
988	$A_g$	2 690	452	131	} $\nu_1(\text{S}^{16}\text{O}_3^{18}\text{O}^{2-})$ $\nu_1(\text{SO}_4^{2-})$
1 088	$F_g$		165		
1 093	$E_g$	28		29	} $\nu_3(\text{SO}_4^{2-})$
1 099	$F_g$		50		
1 120	$F_g$		5		

**Table 11.** Vibrational frequencies and assignments for CsTi(SO<sub>4</sub>)<sub>2</sub>·12H<sub>2</sub>O, between 275 and 1 200 cm<sup>-1</sup>

$\bar{\nu}/\text{cm}^{-1}$		$Z(Y'Y')X'$	$Z(Y'Z)X'$	$Z(X'Y')X'$	Assignment
291	$E_g$			11	} $\nu_3(\text{TiO}_6)$
292	$F_g$	27	27		
325	$F_g$	23	32	3	
346	$A_g$	ca. 3			} $\nu_2(\text{SO}_4^{2-})$ + $\nu_2(\text{TiO}_6)$
436	$E_g$			93	
444	$F_g$	165	167		
458	$F_g$ (?)	ca. 12	ca. 6		} $\nu_1(\text{TiO}_6)$
469	$F_g$	ca. 30	ca. 25		
472	$E_g$			53	} $\rho_6$
517	$A_g$	120	1		
541	$F_g$	42	32		} $\rho_5$
542	$E_g$			31	
576	$E_g$	22		55	} $\nu_4(\text{SO}_4^{2-})$
592	$F_g$	8	10		
610	$F_g$	68	78	5	
628	$F_g$	52	50		} $\rho_4$
630	$E_g$			40	
677	$E_g$			30	} $\rho_3$
679	$A_g$ (?)	12			
725	$F_g$	3	3		} $\rho_2$
754	$A_g$	10			
764	$F_g$	5	3		} ?
776	$E_g$			7	
861	$A_g$	4			} ?
874	$E_g$	3		10	
894	$A_g$	2			} $\rho_1$
942	$E_g$			3	
964	$A_g$	ca. 20			} $\nu_1(\text{S}^{16}\text{O}_3^{18}\text{O}^{2-})$ ?
973	$A_g$	30			
978	$F_g$		4		} ?
981	$E_g$			4	
988	$A_g$	5 607	55	74	} $\nu_1(\text{SO}_4^{2-})$
1 089	$F_g$	100	111	12	
1 096	$E_g$			17	} $\nu_3(\text{SO}_4^{2-})$
1 098	$F_g$	ca. 15	ca. 15		
1 117	$F_g$	5	7		

450 and 500  $\text{cm}^{-1}$  (for example ref. 24) based mainly on an early i.r. study.<sup>25</sup> These estimates of the wavenumber of the totally symmetric stretching mode are shown to be in error. The results from a recent i.r. study of the caesium alums<sup>3</sup> indicate that the antisymmetric metal(III)-water stretch occurs in the same spectral region as the symmetric stretch. Single-crystal vibrational studies of the hexa-aqua-cations of bivalent Ni,<sup>22,26,27</sup> Zn,<sup>22,28</sup> Mg,<sup>22</sup> Fe,<sup>22</sup> and Cu<sup>28</sup> indicate that the corresponding range for the divalent cation-water stretching frequencies is between 360 and 420  $\text{cm}^{-1}$ . The wavenumber difference between the bivalent and trivalent cation-water stretching modes is therefore between 100 and 150  $\text{cm}^{-1}$  rather than the often stated 50  $\text{cm}^{-1}$ . This is significant when calculating differences between the structure and bonding of the bivalent and trivalent hexa-aqua-cations.

### Acknowledgements

We gratefully acknowledge the financial support of the Australian Research Grants Scheme.

### References

- 1 J. K. Beattie, S. P. Best, B. W. Skelton, and A. H. White, *J. Chem. Soc., Dalton Trans.*, 1981, 2105.
- 2 S. P. Best, R. S. Armstrong, and J. K. Beattie, *J. Chem. Soc., Dalton Trans.*, 1982, 1655.
- 3 S. P. Best, R. S. Armstrong, and J. K. Beattie, *Inorg. Chem.*, 1980, **19**, 1958.
- 4 K. I. Petrov, N. K. Bol'shakova, V. V. Kravchenko, and L. D. Ishhakova, *Russ. J. Inorg. Chem. (Engl. Transl.)*, 1970, **15**, 1529.
- 5 N. Strupler, J. Guillermet, J. Hoffelt, and F. Froment, *Bull. Soc. Chim. Fr.*, 1974, 1830.
- 6 J. A. Campbell, D. P. Ryan, and L. M. Simpson, *Spectrochim. Acta, Part A*, 1970, **26**, 2351.
- 7 V. A. Sipachev and A. I. Grisor'ev, *Zh. Strukt. Khim.*, 1969, **10**, 820.
- 8 A. Da Salverira, M. A. Marques, and N. M. Marques, *C. R. Acad. Sci.*, 1961, **252**, 3983.
- 9 R. E. Hester and R. A. Plane, *Inorg. Chem.*, 1964, **3**, 768.
- 10 D. E. Irish and M. H. Brooker, 'Advances in Infrared and Raman Spectroscopy,' eds. R. J. H. Clark and R. E. Hester, Heyden, London, 1976, vol. 2, p. 254.
- 11 S. K. Sharma, *J. Chem. Phys.*, 1974, **61**, 1748.
- 12 D. M. Adams and D. J. Hills, *J. Chem. Soc., Dalton Trans.*, 1978, 782.
- 13 H. H. Eysel and J. Eckert, *Z. Anorg. Allg. Chem.*, 1976, **424**, 68.
- 14 D. A. Johnson and A. G. Sharpe, *J. Chem. Soc. A*, 1966, 798.
- 15 K. Nakamoto, 'Infrared and Raman Spectra of Inorganic and Coordination Compounds,' 3rd edn., Wiley-Interscience, New York, 1978.
- 16 T. E. Jenkins and J. Lewis, *J. Raman Spectrosc.*, 1981, **11**, 1.
- 17 S. P. Best, Ph.D. Thesis, Sydney University, 1983.
- 18 F. Meserole, J. C. Decius, and R. E. Carlson, *Spectrochim. Acta, Part A*, 1974, **30**, 2179.
- 19 S. Montero, R. Schmölz, and S. Haussühl, *J. Raman Spectrosc.*, 1974, **2**, 101.
- 20 S. S. Ti, S. F. A. Kettle, and O. Ra, *J. Raman Spectrosc.*, 1976, **5**, 325.
- 21 S. Haussühl, *Z. Kristallogr., Kristallgeom., Kristallphys., Kristallchem.*, 1961, **116**, 371.
- 22 T. E. Jenkins and J. Lewis, *Spectrochim. Acta, Part A*, 1981, **37**, 47.
- 23 J. P. Hunt and H. Taube, *J. Chem. Phys.*, 1951, **19**, 602.
- 24 M. Falk and O. Knop, 'Water,' ed. F. Franks, Plenum, New York, 1973, vol. 3, ch. 2.
- 25 I. Nakagawa and T. Shimanouchi, *Spectrochim. Acta*, 1964, **20**, 429.
- 26 D. M. Adams and W. R. Trumble, *Inorg. Chim. Acta*, 1974, **10**, 235.
- 27 Y. S. Jain, H. D. Bist, and A. L. Verma, *J. Raman Spectrosc.*, 1974, **2**, 327.
- 28 D. W. James and J. M. Whitnall, *J. Raman Spectrosc.*, 1978, **7**, 225.

Received 25th July 1983; Paper 3/1286